ARTICLE
Journal of Cellular Biochemistry 112:1869–1879 (2011)

Journal of Cellular Biochemistry

The Novel Phloroglucinol PMT7 Kills Glycolytic Cancer Cells by Blocking Autophagy and Sensitizing to Nutrient Stress

Kate Broadley,[1] Lesley Larsen,[2] Patries M. Herst,[1] Robin A.J. Smith,[3] Michael V. Berridge,[1] and Melanie J. McConnell[1*]

[1]*Malaghan Institute of Medical Research, Wellington, New Zealand*
[2]*New Zealand Institute for Plant and Food Research Ltd., Dunedin, New Zealand*
[3]*Department of Chemistry, University of Otago, Dunedin, New Zealand*

ABSTRACT

The switch from oxidative phosphorylation to glycolytic metabolism results in cells that generate fewer reactive oxygen species (ROS) and are resistant to the intrinsic induction of apoptosis. As a consequence, glycolytic cancer cells are resistant to radiation and chemotherapeutic agents that rely on production of ROS or intrinsic apoptosis. Further, the level of glycolysis correlates with tumor invasion, making glycolytic cancer cells an important target for new therapy development. We have synthesized a novel redox-active quinone phloroglucinol derivative, PMT7. Toxicity of PMT7 was in part due to loss of mitochondrial membrane potential in treated cells with subsequent loss of mitochondrial metabolic activity. Mitochondrial gene knockout ρ0 cells, a model of highly glycolytic cancers, were only half as sensitive as the corresponding wild-type cells and metabolic pathways downstream of MET were unaffected in ρ0 cells. However, PMT7 toxicity was also due to a block in autophagy. Both wild-type and ρ0 cells were susceptible to autophagy blockade, and the resistance of ρ0 cells to PMT7 could be overcome by serum deprivation, a situation where autophagy becomes necessary for survival. The stress response class III deacetylase SIRT1 was not significantly involved in PMT7 toxicity, suggesting that unlike other chemotherapeutic drugs, SIRT1-mediated stress and survival responses were not induced by PMT7. The dependence on autophagy or other scavenging pathways makes glycolytic cancer cells vulnerable. This can be exploited by induction of energetic stress to specifically sensitize glycolytic cells to other stresses such as nutrient deprivation or potentially chemotherapy. J. Cell. Biochem. 112: 1869–1879, 2011.

KEY WORDS: MITOCHONDRIAL MEMBRANE POTENTIAL; GLYCOLYTIC METABOLISM; NUTRIENT STRESS; ENERGETIC STRESS; AUTOPHAGY; CELL DEATH

Cancer cells frequently use glycolysis to generate ATP in preference to mitochondrial electron transport (MET), even in the presence of oxygen. First described by Otto Warburg in 1926 and now known as the Warburg effect, aerobic glycolytic metabolism in cancer cells is often due to defective mitochondrial respiration, over-expression of oncogenes, or changes in microenvironmental signals. As a consequence, glycolytic cancer cells produce fewer reactive oxygen species (ROS), since leakage of electrons from mitochondrial electron transport is the major source of electrons for ROS generation. In addition, these cells are resistant to the intrinsic induction of apoptosis due to alterations in mitochondrial Ca^{2+} homeostasis (reviewed in Gogvadze et al. [2008]). As a consequence, glycolytic cancer cells are resistant to radiation and chemotherapeutic agents that rely on production of ROS and/or the induction of apoptosis. Glycolytic cancers are also more invasive, due to the high level of lactate produced during glycolysis, resulting in acidification of the local microenvironment. Further, the level of glycolysis correlates with tumor aggressiveness [Simonnet et al., 2002]. This makes glycolytic metabolism in cancers an important target for new therapy development.

To model glycolytic metabolism in cancer, mitochondrial gene knockout mutants, ρ0 cell derivatives are often used. These cells have lost the entire mitochondrial genome, which encodes key components of the mitochondrial electron transport chain. ρ0 cells contain mitochondria, but cannot perform MET or oxidative phosphorylation, and hence rely entirely on glycolysis for energy production [King and Attardi, 1989]. They use an ADP/ATP gradient to maintain mitochondrial membrane potential, and are resistant to radiation and chemotherapeutics that act through mitochondrial function [Singh et al., 1999; Herst and Berridge, 2006] similar to

Additional Supporting Information may be found in the online version of this article.

*Correspondence to: Melanie J. McConnell, Malaghan Institute of Medical Research, PO Box 7060, Wellington South, Wellington 6242, New Zealand. E-mail: mmcconnell@malaghan.org.nz

Received 8 March 2011; Accepted 10 March 2011 • DOI 10.1002/jcb.23107 • © 2011 Wiley-Liss, Inc.
Published online 23 March 2011 in Wiley Online Library (wileyonlinelibrary.com).

highly glycolytic tumors. While the ρ0 is an extreme model of glycolytic cancer, the ratio of glycolytic to oxidative metabolism varies widely across different cancers and can be as high as 95% [Simonnet et al., 2002].

Whereas a highly glycolytic metabolism can allow cancer cells to survive under oxidative stress or hypoxia, autophagy can be used to survive starvation. Autophagy, in which cellular components are sequestered into phagosomes, degraded and recycled, is used to maintain a balance between synthesis and degradation during development and in times of stress [White and DiPaola, 2009]. While autophagy has historically been described as a death pathway, increasing evidence suggests that many cancer cells require autophagy for survival [Jin and White, 2007], and that autophagy is often induced in response to chemotherapy, where it aids cancer cell survival [Vazquez-Martin et al., 2009; Ren et al., 2010; Liu et al., 2011; Lopez et al., 2011; O'Donovan et al., 2011]. Strategies to target autophagy in combination with chemotherapy have been described and clinical trials have recently been initiated [Amaravadi et al., 2011]. However, autophagy has also been associated with increased sensitivity to chemotherapy and radiation [Lin et al., 2010; Sun et al., 2010], indicating the complexity of autophagy and autophagic cell death in cancer cell survival.

Cancer cell survival is often mediated by SIRT1. This NAD+ dependent deacetylase increasingly appears to be a central mediator of stress responses. It is induced in response to many different stresses, including but not limited to hypoxia, oxidative stress, DNA damage, mitochondrial damage, glucose and serum restriction, aging, and chemotoxic stress. SIRT1 activity and expression are regulated by the metabolic and redox status of the cell resulting in cell survival or death as appropriate (reviewed in Haigis and Sinclair [2010]). SIRT1 has been linked to many diverse cellular processes, including mitochondrial metabolism [Anderson et al., 2008], glycolysis [Rodgers et al., 2005], and autophagy [Lee et al., 2008].

As part of a program to develop redox-active drugs, our groups have designed a series of quinone derivatives with potential anti-tumor activity, based on the mitochondrial-targeted MitoQ [Kelso et al., 2001] These compounds insert a quinone motif derived from co-enzyme Q across the inner leaflet of a membrane bilayer, and the new derivatives have been shown to inhibit electron transport across mitochondrial and plasma membranes at low micromolar concentrations (data not shown). One of these compounds, PMT7, a quinone linked to a weakly acidic phloroglucinol group, was chosen as a candidate for further study. We determined that PMT7 was cytotoxic via two mechanisms, mitochondrial depolarization and autophagy blockade, then demonstrated that by increasing the reliance on autophagy, previously resistant glycolytic cancer cells could be effectively sensitized to PMT7 toxicity.

MATERIALS AND METHODS

SYNTHESIS OF PMT7

1,4-bis(benzyloxy)-2-(10-hydroxydecyl)-5,6-dimethoxy-3-methylbenzene (1). The compound was prepared from 2-(10-hydroxydecyl)-5,6-dimethoxy-3-methyl-1,4-benzenediol [Morimoto, 1989]. A mixture of 2-(10-hydroxydecyl)-5,6-dimethoxy-3-methyl-1,4-benzenediol (7.30 g, 21.4 mmol), benzyl bromide (10.98 g, 64.2 mmol), and potassium carbonate (8.90 g, 64.1 mmol) was refluxed in acetone (150 ml) under a nitrogen atmosphere for 42 h. After cooling, the mixture was diluted with water (150 ml) and extracted with ethyl acetate (2 × 150 ml). The organic phase was washed with saturated brine (150 ml), dried ($MgSO_4$), filtered, and evaporated in vacuo to give a crude product (20 g), which was chromatographed on a silica gel column packed in hexane. Elution with 70% ether/hexane gave the benzyl ether (1).

1,4-bis(benzyloxy)-2-(10-iododecyl)-5,6-dimethoxy-3-methylbenzene (2). To a stirred solution of 1,4-bis(benzyloxy)-2-(10-hydroxydecyl)-5,6-dimethoxy-3-methylbenzene 1 (1.5 g) and triethylamine (0.8 ml) in dichloromethane (50 ml) at RT was added methane sulfonyl chloride (0.245 ml) in DCM (15 ml) dropwise over 15 min. The reaction mixture was stirred for a further 1 h, then diluted with water, extracted with DCM, dried and evaporated in vacuo to give a pale yellow oil. The yellow oil was dissolved in acetone (5 ml) and stirred with sodium iodide (1 g) for 24 h at RT. The mixture was diluted with water (20 ml), extracted into DCM, dried, and evaporated in vacuo to give the product as a yellow oil. Purification by column chromatography over silica gel eluting with 50–100% dichloromethane in 40–60 petroleum ether gave the product as a colorless oil.

2-(10-(2,5-bis(benzyloxy)-3,4-dimethoxy-6-methylphenyl)decyl)benzene-1,3,5-triol (3). A solution of phloroglucinol (0.5 g, 4.0 mmol) and iodide 2 (0.4 g, 0.63 mmol) in methanol (10 ml) containing potassium hydroxide (0.5 g) was heated to 65°C for 4 h. The reaction mixture was diluted with chloroform, washed with water, dried, and the solvents removed in vacuo to give a brown gum. Purification by column chromatography over silica gel eluting with 0–20% methanol in chloroform gave the product 3 as a pale brown gum.

2-(10-(2,4,6-trihydroxyphenyl)decyl)-5,6-dimethoxy-3-methyl-2,5-cyclohexadiene-1,4-dione (PMT7). A solution of the dibenzyloxybenzene 3 (50 mg, 0.08 mmol) in methanol (10 ml) containing Pd/C (10%, 4 mg) was stirred under an atmosphere of hydrogen for 3 h. The mixture was filtered through Celite® in air and the solvents removed in vacuo to give the quinone PMT7 as a yellow gum.

MATERIALS

PMT7 was dissolved in DMSO at 5 mM. WST-1 (2-(4-iodophenyl)-3-(4-nitrophenyl)-5-(2,4-disulfophenyl)-2H-tetrazolium monosodium salt) and PMS (1-methoxy-phenazine methosulfate) were purchased from Dojindo Laboratories (Kumamoto, Japan). All cell culture reagents were purchased from Invitrogen (Auckland, New Zealand). Unless otherwise stated all other reagents were from Sigma Chemical Company (St. Louis, MO).

CELL LINES

HL-60, HeLa, K562, and T98G cells were grown in RPMI-1640 media supplemented with 1% penicillin streptomycin and 5% or 10% (T98G) heat inactivated FBS at 37°C in 5% CO_2. HeLa and HL-60 ρ0 lines were derived by continued culture in 50 ng/ml ethidium bromide, and loss of mitochondrial DNA confirmed by PCR [King and Attardi, 1989]. ρ0 cells were grown in RPMI-1640 media

supplemented with 1% penicillin streptomycin, 1 mM pyruvate, 0.2 mM uridine, and 5% heat inactivated FBS at 37°C in 5% CO_2.

Adherent cells were seeded approximately 16 h prior to the drug treatment, 0.35×10^5 cells/ml (HeLa) or 0.2×10^6 cells/ml (T98G). Cells were approximately 70% confluent on the day of drug treatment. Suspension cells were plated on the day of the drug treatment, 0.4×10^6 cells/ml for all lines. All cells were in exponential growth phase on the day of experiments.

PI EXCLUSION VIABILITY ASSAYS

Cells were collected 24, 48, and 72 h post drug treatment and viability determined by propidium iodide (PI) exclusion, directly measuring the integrity of the cell membrane. Briefly, the cells were rinsed twice with 1× PBS and resuspended at 10^5 cells/ml in PBS + 1% BSA. Prior to analysis, 3.7 μM PI was added and the cells were incubated for 5 min at room temperature. Flow cytometry was performed on a BD FACSort (Becton–Dickinson, San Jose, CA). Ten thousand events were collected and PI fluorescence measured in FL-3H for each sample. The proportion of PI positive non-viable cells were quantified and directly compared.

METABOLIC ASSAYS

MTT reduction was used to measure the level of cytosolic reducing equivalents mainly originating from glycolysis (predominantly NADH). Briefly 100 μl of cells were plated into a 96 well plate—plated either the day prior to the drug for adherent cells, or on the day of drug treatment for suspension cells. At 24, 48, and 72 h post drug treatment 0.45 mg/ml of MTT (3(4,5 dimethylthiozol-2-yl)2,5 diphenyl tetrazolium bromide) in Hanks Buffered Salt Solution (HBSS) was added to each well and incubated at 37°C for 2 h. The cells were lysed with 100 μl of SDS lysing buffer (346 mM SDS, 0.6 mM dimethylformamide pH 4.7) and left overnight for the crystals to dissolve. Endpoint absorbance was measured at 570 nm on a Fluostar Optima plate reader (Fluostar, Berthold, Germany). *WST-1 reduction* was used to measure the level of NADH mainly originating from mitochondrial Krebs cycle activity [Tan and Berridge, 2004]. Briefly, 100 μl of cells were plated into a 96 well plate, either the day prior to the drug (adherent cells), or on the day of drug treatment, (suspension cells). At 24, 48, or 72 h post drug treatment the media was removed and the cells were rinsed twice with 1× HBSS. Dye reduction was initiated by adding 10 μl of a 10× stock solution of WST-1/PMS in MilliQ water (final concentrations of 500 μM WST-1 and 20 μM PMS). WST-1 reduction was measured in real time at 450 nM over 30–60 min in a BMG FLUOstar OPTIMA plate reader (Fluostar, Berthold, Germany) and expressed as a rate, absorbance per minute.

LC3 IMMUNOFLUORESCENCE

Treated cells were cytospun and fixed in 95% ice-cold ethanol: 5% glacial acetic acid for 30 min, then immunocytochemistry performed using an anti-LC3B antibody (Novus Biologicals, Littleton, CO) and an Alexa 647 secondary antibody. A DAPI-containing antifade (Prolong Gold, Invitrogen, New Zealand) was used to protect signal and visualize the nucleus under fluorescent microscopy. Images were obtained using the Olympus B202 fluorescent microscope and Cell^F software (Olympus, New Zealand).

MITOCHONDRIAL MEMBRANE POTENTIAL

After treatment with 50 μM PMT7 for 90 min, cells were incubated with 50 nM MitoTracker Red (Invitrogen, New Zealand) for 30 min at 37°C, and PI added to distinguish dead cells. Emitted fluorescence was measured at 599 nm by flow cytometry on an LSRII SORP cytometer (Becton–Dickinson, San Jose, CA).

MITOCHONDRIAL SUPEROXIDE MEASUREMENT

Cells were incubated with 5 μM MitoSOX (Invitrogen, Auckland, New Zealand) for 10 min, then fluorescence measured at 580 nm on a LSR2 cytometer (Becton–Dickinson, San Joe, CA).

SIRT1 ACTIVITY

Cells were serum starved (0.1% FBS) for 48 h prior to cell collection. Histone protein was collected from $2–3 \times 10^6$ cells. Cells were washed twice in PBS and resuspended in lysis buffer (10 mM Tris, 50 mM Mg_2SO_4, 1% Triton X-100, 5 mM $MgCl_2$, 250 mM sucrose, pH 6.5) to isolate the nuclear fraction, which was pelleted by centrifugation. Histones were isolated from the nuclear fraction by a 3 h acid extraction (100 μl of 10 mM Tris-HCl, 13 mM EDTA, pH7.4; 1.1 μl of concentrated H_2SO_4) followed by an overnight incubation with 1 ml of 100% acetone overnight hours at 4°C to precipitate, then pelleted by centrifugation and dissolved in water. Protein was quantified using the DC assay (Bio-Rad, Auckland, New Zealand). Twenty micrograms of purified histones were separated by 15% SDS–PAGE and transferred to PVDF membrane (BioRad, Auckland, New Zealand). The membrane was stained with 0.1% Amido black and digitally scanned. After blocking in 3% skim milk/PBS at room temperature, the membrane was incubated with 1:2,000 dilution (3% skim milk/PBS) of an antibody against histone 4-lysine 16-acetyl (Millipore, North Ryde, Australia). An HRP-conjugated goat anti-rabbit IgG secondary antibody was used at 1:5,000 dilution (3% skim milk/PBS). Detection of protein was performed by enhanced chemiluminescence (Supersignal ECL kit, Pierce) and autoradiography (Kodak X-Omat, Kodak, NY).

SIRT1 INHIBITION AND KNOCKDOWN

Cells were exposed to 10 mM nicotinamide dissolved in PBS for inhibition assays. Knockdown of SIRT1 was carried out with a shRNA construct targeting either SIRT1 (AAG ATG AAG TTG ACC TCC TCA [Picard et al., 2004]) or luciferase cloned into the pSIREN ZSGreen vector (Clontech, CA). Transfection of HeLa cells was carried out using lipofectamine LTX system (Invitrogen, Auckland, New Zealand) following the manufacturers instructions. Cells were plated out in antibiotic free media the day prior to transfection. On the day of transfection, cells were 60–70% confluent. Transfection complex was added to the cells (500 μl of RPMI-1640, 2.5 μg of plasmid, 3.75 μl of lipofectamine LTX Reagent) and after 3 h incubation, removed and replaced by complete media (RPMI-1640, 5% FBS, 1% pencillin streptomycin). Knock down was measured at 24, 48, and 72 h post transfection by QRT-PCR and Western blot.

SIRT1 WESTERN BLOT

SIRT1 protein was extracted into a lysis buffer (140 mM NaCl, 50 mM Tris pH 7.5–8, 1% triton and protease inhibitor cocktail (Complete EDTA free, Roche, New Zealand)) and quantified using the

DC assay (Bio-Rad, New Zealand). One hundred microgram of total protein was loaded onto a 10% SDS PAGE, electrophoresed, and transferred to PVDF membrane (Bio-Rad, CA). The membrane was stained with 0.1% Amido black and was digitally scanned. After blocking in 3% skim milk at room temperature, the membrane was incubated with 1:200 dilution (3% skim milk) of anti-SIRT1 (Santa Cruz, CA) polyclonal antibody. The secondary antibody used was a goat anti-rabbit IgG HRP (Santa Cruz, CA) at 1:5,000 dilution (3% skim milk). Detection of protein was performed by enhanced chemiluminescence (Supersignal ECL kit, Pierce) and autoradiography (Kodak X-Omat, Kodak, NY) and quantified using ImageJ.

SIRT1 INTRACELLULAR STAINING

Five million transfected cells (shSIRT or shLUC) were fixed in for 30 min in 2% paraformaldehyde/PBS at 4°C, permeabilized in 0.1% TritonX-100 for 2 min on ice, then resuspended in 100 ml of 1% BSA/PBS. SIRT1 was labeled with polyclonal primary antibody, and an anti-rabbit-R-PE secondary antibody, then analyzed by flow cytometry using a LSRII SORP cytometer (Becton–Dickinson, San Jose, CA). All transfected FL1+ cells were gated using a non-transfected control, and the highly transfected cell population defined as the top 20% of FL1 + green fluorescent cells.

RESULTS

SYNTHESIS OF PMT7

As part of a programme to develop novel metabolic drugs, a series of quinone derivatives were designed. One of these, PMT7, displayed strong electron transport inhibition and was chosen as a candidate for further study. It is a weakly acidic phloroglucinol group attached by a ten-carbon chain to the quinone motif from Co-enzyme Q (Fig. 1A). PMT7 was synthesized by alkylation of the protected idenbenol iodide (1) with phloroglucinol to give the adduct (2), followed by deprotection by catalytic hydrogenation and oxidation of the hydroquinol in air to give the quinone (3) (Supporting information and Supp Fig. 1). The iodide (1) was prepared from the known compound idebenol [Morimoto, 1989] by selective benzyl protection of the ring hydroxyls followed by mesylation and subsequent displacement with iodide at the terminal position.

PMT7 PREFERENTIALLY KILLED CELLS DEPENDENT ON MITOCHONDRIAL ELECTRON TRANSPORT

PMT7 was titrated to identify a dose with anti-metabolic activity (WST1 and MTT reduction) in HL60 cells (data not shown). Accordingly, HL-60, HeLa, K562, and T98G cells were each exposed to 50 μM PMT7 or the equivalent concentration of DMSO as a vehicle control. The effect of 24, 48, and 72 h exposure to PMT7 on the viability of these cell lines was determined by accumulation of PI^+ cells and a corresponding decrease in cell number (Fig. 1B). At 50 μM, lines showed differential sensitivity to PMT7; most sensitive were HL-60 and K562, with a five-fold increase in PI^+ cells, and a significant decrease in cell number after 48 h. Forty hour exposure to PMT7 in HeLa cells resulted in 40% increase in PI^+ cells and a 40% decrease in total cell numbers. T98G cells were most resistant to PMT7; the 48 h exposure only marginally increased the number of PI^+ cells without any decrease in cell number.

Interestingly, the sensitivity to PMT7 reflected the main ATP generating pathway of each cell line. Resistant T98G cells predominantly use aerobic glycolysis to generate ATP, while HL60 and K562 rely almost entirely on MET and oxidative phosphorylation (Supp Fig. 2 and [Herst and Berridge, 2007]). Highly glycolytic solid tumors are very aggressive and resistant to many forms of chemotherapy [Simonnet et al., 2002; Kunkel et al., 2003]. We investigated whether highly glycolytic tumor cells were resistant to PMT7 compared to non-glycolytic cells.

Purely glycolytic cells can be artificially derived by prolonged exposure of wild-type cells to low concentrations of ethidium bromide, which intercalates mitochondrial (mtDNA) preferentially to nuclear DNA and prevents replication of the mitochondrial genome [King and Attardi, 1989]. As mtDNA encodes components of the mitochondrial electron transport chain, mtDNA knockout mutants (ρ0 cells) cannot carry out mitochondrial electron transport (MET) and are unable to perform oxidative phosphorylation. ρ0 cells are therefore completely reliant on glycolysis for generation of ATP. We compared the effect of PMT7 on the number of PI^+ cells in both HeLa and HL60 parental and ρ0 cells. Both ρ0 cell lines were only half as sensitive as their corresponding parental cells to PMT7 (Fig. 1C).

PMT7 DEPOLARIZED MITOCHONDRIAL MEMBRANE POTENTIAL

As NADH flux is regulated to a large extent by mitochondrial activity, we determined the effect of PMT7 on mitochondrial membrane potential (MMP). ρ0 cells maintain MMP with an ATP/ADP gradient [Appleby et al., 1999] rather than the proton gradient generated by MET in wild-type cells. Sensitive parental and resistant ρ0 cells were treated with the rosamine dye MitoTracker Red (MTR), accumulation of which indicates active mitochondrial membrane potential. Mitochondria of both parental and ρ0 HL60 cells were depolarized by PMT7 by greater than 90%, as shown by the loss of MTR fluorescence (Fig. 2A), as were wild-type and ρ0 HeLa cells (data not shown). This demonstrated that PMT7 depolarizes mitochondria and dissipates membrane potentials, regardless of origin, indicating loss of integrity of the mitochondrial membrane.

PMT7 REDUCED CYTOSOLIC NADH FLUX IN MET-DEPENDENT CELLS

We next examined the effect of PMT7 on cellular metabolism. The tetrazolium dyes MTT and WST-1/PMS are reduced by NADH—we have shown previously that MTT is reduced intra-cellularly by NADH produced during glycolysis, while the cell impermeable WST-1/PMS is reduced by NADH that was produced predominantly in the TCA cycle, then transferred to the cytosol via the malate-aspartate shuttle [Tan and Berridge, 2004]. Transfer of electrons from this NADH pool via a short electron transport system across the plasma membrane results in the extracellular reduction of WST-1/PMS [Berridge et al., 2005]. Both MTT reduction and WST-1/PMS reduction decreased in the parental cell lines after PMT7 exposure (HeLa, Fig. 2A and HL-60, data not shown). MTT and WST-1/PMS reduction in the glycolytic HeLa ρ0 cells (Fig. 2B) and T98G cells (data not shown) were unaffected by PMT7, suggesting PMT7 decreased TCA cycle activity.

In cells that use MET to generate ATP, the major mitochondrial ROS is superoxide. We measured superoxide in mitochondria before

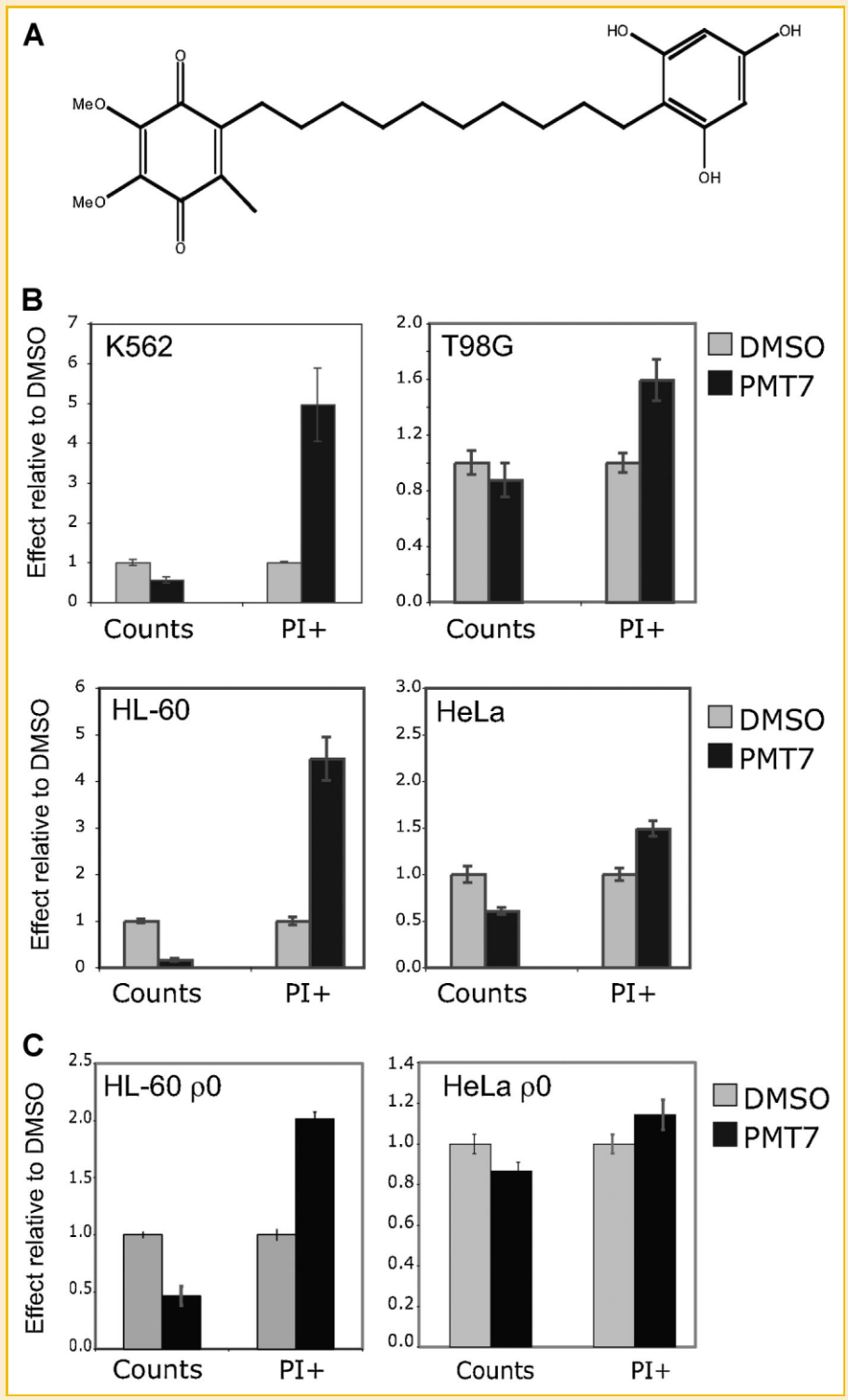

Fig. 1. PMT7 selectively kills cancer cell lines. A: Structure of PMT7. B: Wild-type and (C) ρ0 cell lines were exposed to 50 μM PMT7 and sensitivity determined by the number (total cell counts) and viability (PI exclusion) of surviving cells at 48 h. Results from PMT7-treated cells (black) were normalized to results from vehicle control DMSO-treated cells (light gray). Data are averages ± SD of at least three triplicate experiments.

and after PMT7 exposure (Fig. 2C). Both HL-60 and HeLa wild-type cells expressed much higher superoxide levels than the corresponding ρ0, consistent with lack of MET in ρ0 cells. HL60, more sensitive than HeLa to PMT7, had a much higher basal level of mitochondrial superoxide. PMT7 exposure doubled mitochondrial superoxide in HL60 cells, and increased it five-fold in HeLa cells. PMT7 had no effect on superoxide in ρ0 cells, indicating that superoxide production after PMT7 exposure was dependent on MET.

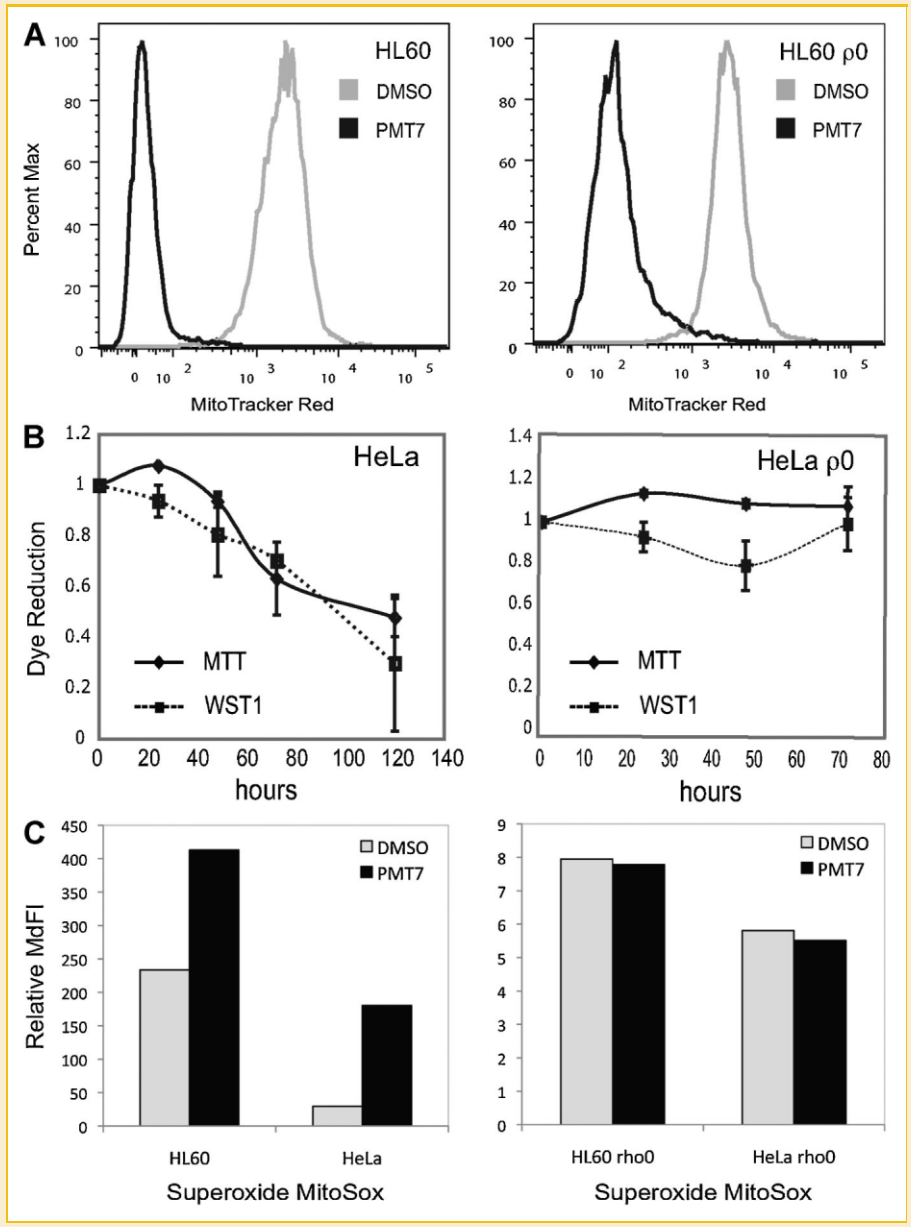

Fig. 2. PMT7 changes mitochondrial activity. A: Cells were exposed to DMSO (gray) or 50 μM PMT7 (black) for 90 min, incubated with MitoTracker Red and fluorescence analyzed by flow cytometry. Data are representative of at least two independent triplicate experiments. B: The effect of 50 μM PMT7 on MTT (black line) and WST1 (dotted line) reduction was measured over time. At each time-point PMT7 was normalized to DMSO, with the zero time-point set to 1. Data are averages ± SEM of triplicate experiments. C: Cells were exposed to DMSO (gray) or 50 μM PMT7 (black) for 90 min, incubated with 5 μM MitoSOX, and fluorescence analyzed by flow cytometry. Data are median fluorescence intensity, and are representative of at least two independent triplicate experiments.

PMT7 BLOCKED AUTOPHAGY

In the course of these experiments, we noted that PMT7-treated cells contained a sub-population characterized by increased side-scatter (SSC^{hi}) and decreased forward scatter (FSC^{lo}), which became more prominent over time (Fig. 3A). The SSC^{hi} population had a greater proportion of PI^+ cells (14.7% PI^+ for SSC^{hi} versus 1.9% PI^+ for SSC^{lo}, Fig. 3B), confirming reduced viability of SSC^{hi} cells.

The relationship between increasing SSC (cytoplasmic complexity, or vesicles) and death suggested involvement of autophagy in the PMT7 response. We examined the effect of PMT7 on the microtubule-associated protein 1 Light Chain 3 (MAP1LC3, or LC3) by fluorescence microscopy. We observed accumulation of LC3 into large punctae after PMT7 exposure (Fig. 3C), suggesting a block in autophagy. To confirm this we compared PMT7 to 3MA, an autophagy inhibitor. Treatment of HL60 and HeLa cells with 5 μM 3MA led to a similar increase in SSC^{hi} cells (Fig. 3D) as PMT7, supporting the "blocked autophagy" phenotype of SSC^{hi} cells. Further, the combination of 3MA and PMT7 was no more than additive on the SSC^{hi} population, supporting the hypothesis that

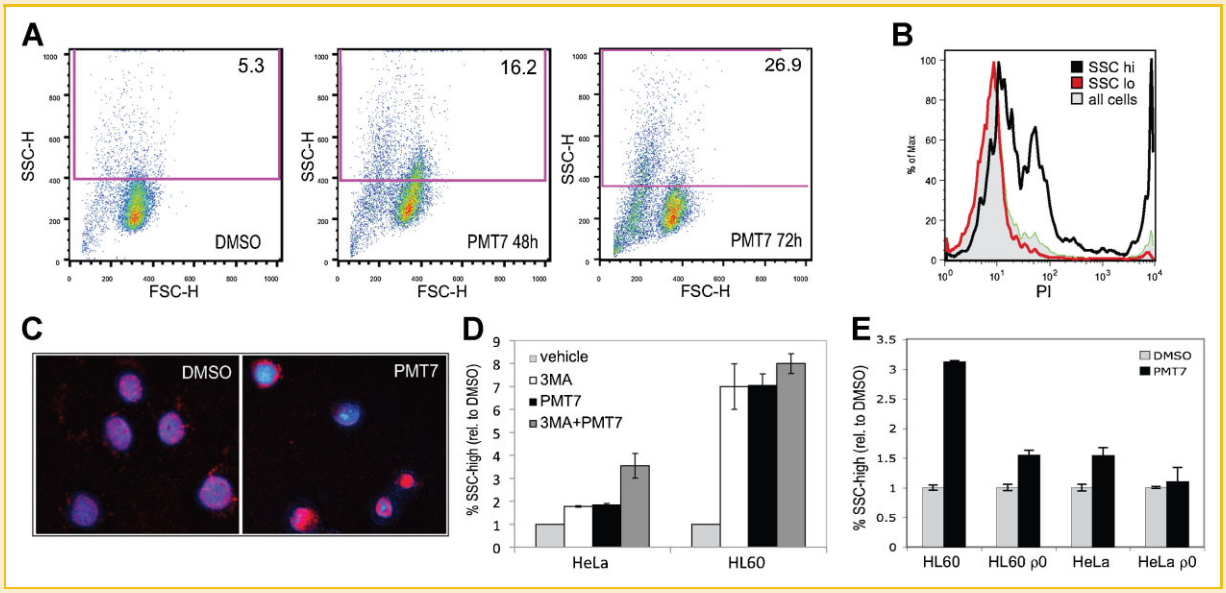

Fig. 3. PMT7 blocks autophagy. A: HL60 cells were treated with 50 μM PMT7 or the equivalent amount of DMSO for 48 and 72 h. SSC^{hi} gate was set on 48 h DMSO-treated cells and applied to all samples. Data shown are representative of at least three independent experiments. Percentage of population in SSC^{hi} gate is stated. B: The 72 h PMT7 sample from (A) was analyzed. The SSC^{lo} gate was defined below the SSC^{hi} gate from (A). PI fluorescence was measured in FL3-H and the SSC^{hi} (black line) and SSC^{lo} (red line) cells compared to the combined profile (shaded gray histogram). C: HL-60 cells were treated with PMT7 or DMSO for 48 h and cytospun onto glass slides. Cells were fixed, permeabilized and stained with an anti-LC3 antibody and R-PE-labeled secondary antibody. Nuclei were visualized with DAPI, and cells examined by fluorescence microscopy. D: HL60 and HeLa cells were exposed to DMSO (gray), 5 mM 3MA (white), 50 μM PMT7 (black) or the combination of 3MA and PMT7 (dark gray) for 48 h then analyzed by flow cytometry. The percentage of SSC^{hi} cells in the treatment groups was expressed relative to the percentage in the DMSO control, which was normalized to 1. Data are averages ± SD of at least two independent triplicate experiments. E: Wild-type and ρ0 cells were exposed to DMSO (gray) or 50 μM PMT7 (black) then percentage of SSC^{hi} cells in PMT7 treatment determined by flow cytometry, and expressed relative to the percentage in the DMSO control, which was normalized to 1. Data are averages ± SD of at least two independent triplicate experiments.

PMT7 acts on the same pathway as 3MA, blocking autophagic cell death.

We compared SSC^{hi} induction in response to PMT7 between the sensitive wild-type and resistant ρ0 cells. In HL60 ρ0 cells treated with 50 μM PMT7 for 48 h, the number of SSC^{hi} cells increased by 50%, compared with 300% in wild-type cells (Fig. 3E). The SSC^{hi} population increased by 50% with PMT7 treatment of wild-type HeLa cells. This was less than HL60, consistent with the reduced sensitivity of HeLa cells. Again, PMT7 did not increase the HeLa ρ0 SSC^{hi} population at all (Fig. 3E). Changes in SSC^{hi} were consistent with the effect of PMT7 on viability, MTT/WST-1 reduction, and superoxide production of both wild-type and ρ0 cells.

Taken together, these data suggest two mechanisms of PMT7 toxicity. Depolarization of mitochondria was directly cytotoxic to wild-type cells due to loss of MET and subsequent ATP generation, with the associated production of mitochondrial superoxide. Purely glycolytic ρ0 cells were resistant to mitochondrial depolarization, because they do not use MET to generate energy. The second mechanism is based on the ability of PMT7 to prevent completion of autophagy, which would reduce nutrient recycling. Both wild-type and ρ0 cells were susceptible to autophagy blockade.

ρ0 RESISTANCE IS OVERCOME BY NUTRIENT STARVATION

If PMT7 blocks autophagy, then cells with an increased requirement for autophagy should be more sensitive to PMT7 toxicity. Serum starvation increases autophagy [Gozuacik and Kimchi, 2004], so PMT7 toxicity was measured in serum-depleted cells. Wild-type and ρ0 HL-60 and HeLa cells were transferred to 10% or 0.1% FBS for 48 h, with 25 μM PMT7 added for the final 24 h, half the dose and incubation time used in the original cytotoxicity assays. Cell death was measured by accumulation of PI-positive cells at 24 h. This sub-optimal exposure did not induce significant death in either cell line in serum-replete conditions, but in serum-starved HL60 and HeLa cells death increased five-fold after PMT7 treatment (Fig. 4A). As predicted by our autophagy blockade model, serum-starved ρ0 cells also became sensitive to PMT7. Accumulation of PI^{+} serum-starved ρ0 cells after PMT7 was equivalent to that of wild-type cells, demonstrating that resistant glycolytic cells could be rendered sensitive to PMT7 under nutrient starvation. The basal level of SSC^{hi} cells increased in starved cells (data not shown), suggesting the onset of autophagy was sufficient to render the resistant ρ0 cells sensitive to PMT7 autophagy blockade. Similarly, PMT7 in combination with the autophagy blocker 3MA also increased death of ρ0 cells by PMT7, although to a lesser extent (data not shown).

SIRT1 LOSS DID NOT SIGNIFICANTLY ALTER PMT7 ACTIVITY

The deacetylase SIRT1 is activated by many stresses, including ROS and serum starvation; SIRT1 activity is regulated in part by the $NADH/NAD^{+}$ ratio. This has led to the description of SIRT1 as a critical sensor of metabolic and energetic stress [Feige et al., 2008; Canto et al., 2009], and a mediator of stress responses [Saunders and Verdin, 2007; Haigis and Sinclair, 2010]. With PMT7 alteration of

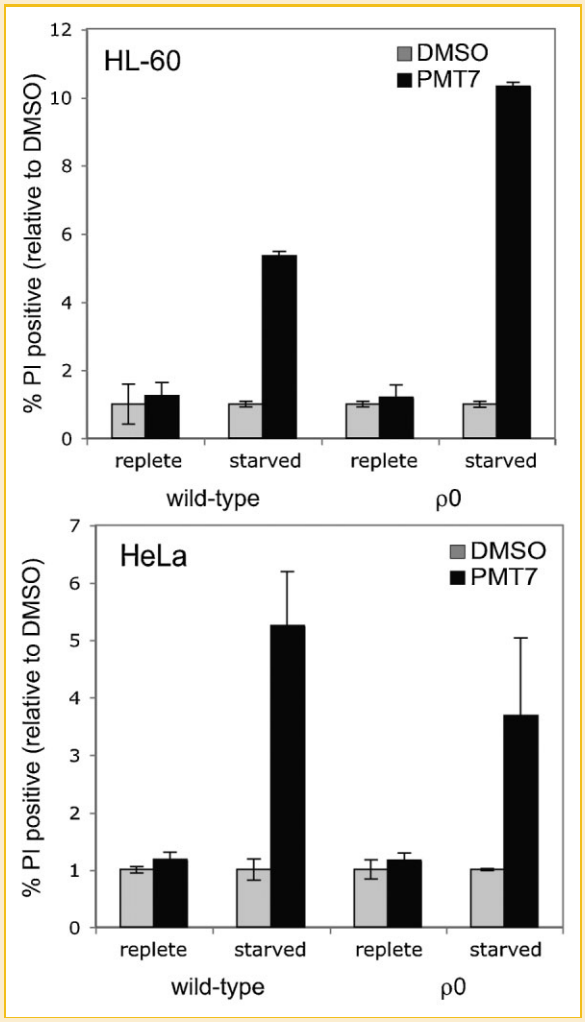

Fig. 4. Serum starvation increases toxicity of PMT7. Cells were grown in either 10% serum (replete) or transferred to 0.1% serum for 24 h, then exposed to DMSO (gray) or 50 μM PMT7 (black) for 24 h. PI exclusion analysis was performed by flow cytometry at 48 h. PMT7 (black) was normalized to the vehicle control DMSO (gray). Data are averages ± SD of at least three triplicate experiments.

NADH metabolism and mitochondrial ROS, and the increased sensitivity of serum-starved cells, we asked whether there was a role for SIRT1 in PMT7 cytotoxicity. As previously reported [Vaquero et al., 2006], SIRT1 deacetylase activity on the histone substrate H4K16 was increased under serum starvation in all cells tested (Fig. 5A). Wild-type and ρ0 cells were serum-starved as above and 10 mM nicotinamide (NAM) was used to inhibit SIRT1. This had no effect on PMT7 cytotoxicity, either against serum-replete or serum-starved cells (Fig. 5B and data not shown), despite the increased SIRT1 activity in starved cells. This was confirmed by shRNA knockdown of SIRT1 [Picard et al., 2004]. An average 40% decrease in SIRT1 protein was measured by Western blot (Fig. 5C, left), which included a population of highly transfected cells with significant loss of SIRT, as determined by flow cytometry (Fig. 5C, right). Consistent with NAM inhibition, SIRT1 knockdown had no effect on cytotoxicity of PMT7 (Fig. 5D, left). Even when only the highly transfected cells with the greatest loss of SIRT1 were analyzed, PMT7 cytotoxicity was not significantly affected (Fig. 5D, right).

DISCUSSION

Cytotoxic activity of the novel phloroglucinol PMT7 was demonstrated across a variety of cancer cell lines, particularly those who rely on MET for energy production [Herst and Berridge, 2007]. Highly glycolytic GBM cell lines, and constitutively glycolytic ρ0 cell lines were more resistant. Although PMT7 blocked autophagy, and rapidly depolarized mitochondria in all cells, this increased mitochondrial superoxide production and decreased cytosolic NADH flux in sensitive cells only. Despite mitochondrial depolarization in PMT7-resistant ρ0 cells, PMT7 did not change NADH flux or increase superoxide production in ρ0 cells, and was only half as toxic as in wild-type cells. These results imply a dual mechanism of action for PMT7, with autophagy blockade independent from the mitochondrial depolarization and subsequent loss of MET and oxidative phosphorylation. Like other quinone-containing compounds, the ubiquinone motif of PMT7 is probably responsible for the loss of mitochondrial membrane potential, although we have not formally demonstrated this.

The resistance of ρ0 cells to PMT7 could be overcome by serum deprivation, a situation where autophagy becomes necessary for survival. Starved ρ0 cells did not survive PMT7; presumably blocking autophagy led to an inability to recycle nutrients and access enough glucose [Kotoulas et al., 2006] to sustain the high levels of glycolysis needed for continued glycolytic energy production. Thus, in highly glycolytic cells, starvation leads to energy stress, and potentially subsequent sensitization to other stresses.

We demonstrated that serum deprivation increased both PMT7 toxicity, and activity of the class III deacetylase SIRT1. However, inhibition with NAM, and knockdown experiments showed that loss of SIRT1 did not significantly alter PMT7-mediated cell death. This was unexpected, since SIRT1 has been proposed to enhance survival of cells under chemotoxic stress [Matsushita et al., 2005; Oh et al., 2010] and has important roles in starvation [Nemoto et al., 2004] and autophagy induction [Lee et al., 2008; Hariharan et al., 2010]. This may be related to the transient knockdown of SIRT1, although the absence of a NAM-mediated effect on cell death supports the lack of SIRT1 involvement. We concluded that while starvation increased PMT7 toxicity, it was not mediated through increased SIRT1 activity, and was more likely due to the increased requirement for autophagy in starved cells.

Nutrient stress has many consequences for cellular metabolism, such as slower proliferation rates and up-regulation of survival pathways. Unlike many other cytotoxic drugs, PMT7 toxicity was not affected by the lower proliferation rate of serum-starved cells, suggesting that PMT7 and similar compounds might be active against relatively quiescent cells. Similarly, the lack of significant involvement of SIRT1 suggests that PMT7 does not induce survival pathways mediated by SIRT1. This opens the potential use of PMT7 and derivatives to target populations of cells that may be resistant to

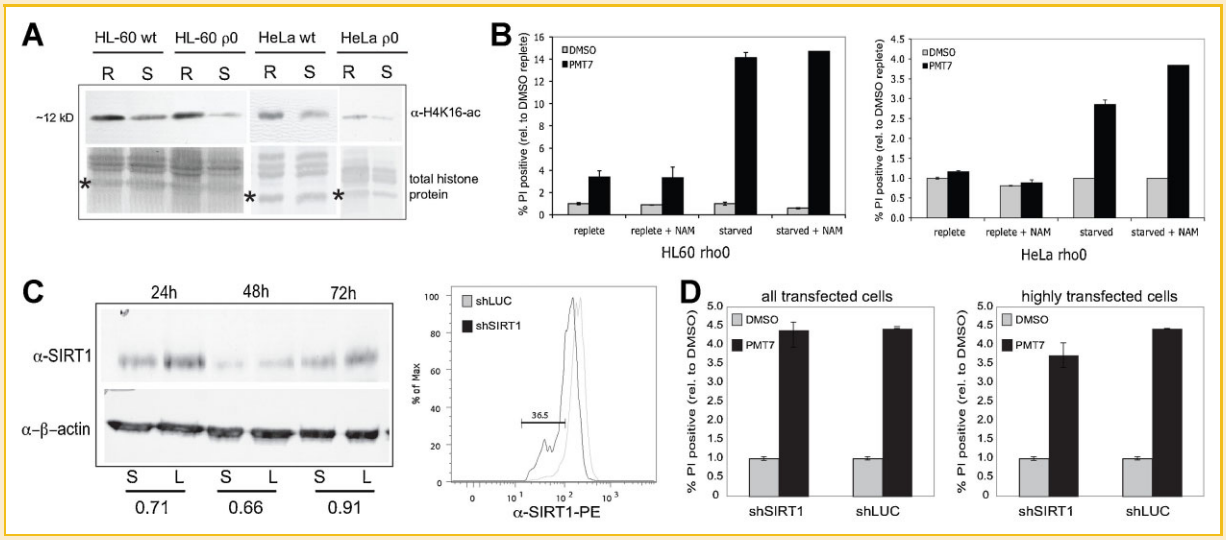

Fig. 5. SIRT1 is not necessary for enhanced PMT7 toxicity in starved cells. A: Cell lines were grown in serum-replete (R) or 0.1% serum (S) for 48 h. Histone proteins were acid-extracted, precipitated with acetone and separated by SDS–PAGE. Acetylation of histone 4 lysine 16 was determined by western blotting with a specific antibody (upper panel). Membrane was stained with amido black to visualize total acid-extracted protein and used as a loading control (lower panel). Histone 4 band indicated with asterisk. B: ρ0 cells were grown in either 10% serum (replete) or transferred to 0.1% serum for 24 h, then exposed to DMSO (gray), 10 mM NAM, or 50 μM PMT7 (black) as described, then PI exclusion analysis performed by flow cytometry at 48 h. All data were normalized to the serum-replete, +DMSO, -NAM control. Data are averages ± SD of at least three triplicate experiments. C: HeLa cells were transfected with a short hairpin RNAi construct targeting either SIRT1 (S) or firefly luciferase (L). Cells were lysed at 24, 48, and 72 h and soluble proteins separated by SDS-PAGE. Protein was transferred to PVDF membrane and SIRT1 and b-actin visualized by western blot. Blots were scanned, SIRT1 was quantified relative to b-actin, and the reduction in SIRT1 protein after knockdown calculated using densitometry analysis. Number shows the average reduction from three independent experiments. D: HeLa cells were transfected with short hairpin RNAi targeting either luciferase (shLUC) or SIRT1 (shSIRT1), and incubated with 50 μM PMT7 for 48 h. The FL1+ transfected cells (left panel) or $FL1^{hi}$ highly transfected cells (right panel) were gated, the percentage of PI^{+} cells in the DMSO or PMT7-treated ShLUC and shSIRT1 cells determined, and PMT7 expressed relative to DMSO. Data are averages ± SD of at least two independent triplicate experiments.

traditional therapies due to quiescence or stress resistance mechanisms, such as cancer stem cells.

The increased susceptibility of highly glycolytic cells to other treatments while under nutrient stress is consistent with our recently published clinical data. Patients with highly glycolytic leukaemic blasts survived significantly longer after treatment than patients whose leukemic blasts had moderate or low levels of glycolytic metabolism [Herst et al., 2011]. Increased sensitivity of glycolytic leukemia to different forms of chemotherapy was in stark contrast to data from solid tumors, where highly glycolytic tumors are more resistant to treatment. We hypothesize that this is due to limited nutrient resources in the leukemia cell bone marrow niche, compared with solid tumors with their increased vasculature and blood supply. While highly glycolytic leukaemic blasts may already be under nutrient stress, glycolytic solid tumors could be made vulnerable by blocking autophagy or other scavenging pathways with PMT7 or similar agents.

Highly glycolytic solid tumors are often aggressive and invasive [Simonnet et al., 2002; Kunkel et al., 2003], as well as radiation and chemotherapy resistant [Gatenby and Gillies, 2007; Moreno-Sanchez et al., 2007; Gillies et al., 2008]. Cancer cell killing by direct inhibition of glycolysis has been studied for decades [Bicz and Broniszewska-Ardelt, 1967; Floridi et al., 1981; Liu et al., 2001; Ganapathy-Kanniappan et al., 2010], but will target normal cells that also depend exclusively on glycolysis for energy production, such as rapidly proliferating T-cells [Wang et al., 1976]. Induction of energetic stress, while making glycolytic cancer cells more vulnerable, could potentially leave normal cells unharmed, since they may be less dependent on salvage and scavenging pathways. While PMT7 is not an ideal drug, with relatively high concentrations needed for maximum efficacy, it demonstrates the successful combination of energetic stress (autophagy blockade) with nutrient stress (serum deprivation) for highly glycolytic tumors, and provides a lead compound to derive new drugs from. By exploiting a weakness of glycolytic cells—the requirement for recycling and salvage pathways such as autophagy for survival—rather than directly targeting glycolysis, these data suggest a new approach to combat these otherwise resistant, aggressive cancers.

ACKNOWLEDGMENTS

The authors thank An Tan for helpful discussions and Dr. Abdul Rahman bin Manas for the supply of precursor chemicals. KB was supported by grant GOT-0623-RPG from the Genesis Oncology Trust to MJM. PMT7 was produced under grants from the Cancer Society of New Zealand and the Genesis Oncology Trust to RAJS and MB. MJM was the Sir Roy McKenzie Medical Research Fellow at the Malaghan Institute of Medical Research. Funding bodies had no involvement in study design, data collection or analysis, or writing and submission of the manuscript.

REFERENCES

Amaravadi RK, Lippincott-Schwartz J, Yin XM, Weiss WA, Takebe N, Timmer W, Dipaola RS, Lotze MT, White E. 2011. Principles and current strategies for targeting autophagy for cancer treatment. Clin Cancer Res 17:654–666.

Anderson RM, Barger JL, Edwards MG, Braun KH, O'Connor CE, Prolla TA, Weindruch R. 2008. Dynamic regulation of PGC-1alpha localization and turnover implicates mitochondrial adaptation in calorie restriction and the stress response. Aging Cell 7:101–111.

Appleby RD, Porteous WK, Hughes G, James AM, Shannon D, Wei YH, Murphy MP. 1999. Quantitation and origin of the mitochondrial membrane potential in human cells lacking mitochondrial DNA. Eur J Biochem 262:108–116.

Berridge MV, Herst PM, Tan AS. 2005. Tetrazolium dyes as tools in cell biology: new insights into their cellular reduction. Biotechnol Annu Rev 11:127–152.

Bicz W, Broniszewska-Ardelt B. 1967. 2-deoxy-D-glucose as an inhibitor of the metabolism of tumor cells. Arch Immunol Ther Exp (Warsz) 15:112–114.

Canto C, Gerhart-Hines Z, Feige JN, Lagouge M, Noriega L, Milne JC, Elliott PJ, Puigserver P, Auwerx J. 2009. AMPK regulates energy expenditure by modulating NAD+ metabolism and SIRT1 activity. Nature 458:1056–1060.

Feige JN, Lagouge M, Canto C, Strehle A, Houten SM, Milne JC, Lambert PD, Mataki C, Elliott PJ, Auwerx J. 2008. Specific SIRT1 activation mimics low energy levels and protects against diet-induced metabolic disorders by enhancing fat oxidation. Cell Metab 8:347–358.

Floridi A, Paggi MG, Marcante ML, Silvestrini B, Caputo A, De Martino C. 1981. Lonidamine, a selective inhibitor of aerobic glycolysis of murine tumor cells. J Natl Cancer Inst 66:497–499.

Ganapathy-Kanniappan S, Vali M, Kunjithapatham R, Buijs M, Syed LH, Rao PP, Ota S, Kwak BK, Loffroy R, Geschwind JF. 2010. 3-bromopyruvate: a new targeted antiglycolytic agent and a promise for cancer therapy. Curr Pharm Biotechnol 11:510–517.

Gatenby RA, Gillies RJ. 2007. Glycolysis in cancer: a potential target for therapy. Int J Biochem Cell Biol 39:1358–1366.

Gillies RJ, Robey I, Gatenby RA. 2008. Causes and consequences of increased glucose metabolism of cancers. J Nucl Med 49(Suppl 2):24S–42S.

Gogvadze V, Orrenius S, Zhivotovsky B. 2008. Mitochondria in cancer cells: what is so special about them? Trends Cell Biol 18:165–173.

Gozuacik D, Kimchi A. 2004. Autophagy as a cell death and tumor suppressor mechanism. Oncogene 23:2891–2906.

Haigis MC, Sinclair DA. 2010. Mammalian sirtuins: biological insights and disease relevance. Annu Rev Pathol 5:253–295.

Hariharan N, Maejima Y, Nakae J, Paik J, Depinho RA, Sadoshima J. 2010. Deacetylation of FoxO by Sirt1 plays an essential role in mediating starvation-induced autophagy in cardiac myocytes. Circ Res 107:1470–1482.

Herst PM, Berridge MV. 2006. Plasma membrane electron transport: a new target for cancer drug development. Curr Mol Med 6:895–904.

Herst PM, Berridge MV. 2007. Cell surface oxygen consumption: a major contributor to cellular oxygen consumption in glycolytic cancer cell lines. Biochim Biophys Acta 1767:170–177.

Herst PM, Howman RA, Neeson PJ, Berridge MV, Ritchie DS. 2011. The level of glycolytic metabolism in acute myeloid leukemia blasts at diagnosis is prognostic for clinical outcome. J Leukoc Biol 89:51–55.

Jin S, White E. 2007. Role of autophagy in cancer: management of metabolic stress. Autophagy 3:28–31.

Kelso GF, Porteous CM, Coulter CV, Hughes G, Porteous WK, Ledgerwood EC, Smith RA, Murphy MP. 2001. Selective targeting of a redox-active ubiquinone to mitochondria within cells: antioxidant and antiapoptotic properties. J Biol Chem 276:4588–4596.

King MP, Attardi G. 1989. Human cells lacking mtDNA: repopulation with exogenous mitochondria by complementation. Science 246:500–503.

Kotoulas OB, Kalamidas SA, Kondomerkos DJ. 2006. Glycogen autophagy in glucose homeostasis. Pathol Res Pract 202:631–638.

Kunkel M, Reichert TE, Benz P, Lehr HA, Jeong JH, Wieand S, Bartenstein P, Wagner W, Whiteside TL. 2003. Overexpression of Glut-1 and increased glucose metabolism in tumors are associated with a poor prognosis in patients with oral squamous cell carcinoma. Cancer 97:1015–1024.

Lee IH, Cao L, Mostoslavsky R, Lombard DB, Liu J, Bruns NE, Tsokos M, Alt FW, Finkel T. 2008. A role for the NAD-dependent deacetylase Sirt1 in the regulation of autophagy. Proc Natl Acad Sci USA 105:3374–3379.

Lin CI, Whang EE, Donner DB, Du J, Lorch J, He F, Jiang X, Price BD, Moore FD Jr, Ruan DT. 2010. Autophagy induction with RAD001 enhances chemosensitivity and radiosensitivity through Met inhibition in papillary thyroid cancer. Mol Cancer Res 8:1217–1226.

Liu H, Hu YP, Savaraj N, Priebe W, Lampidis TJ. 2001. Hypersensitization of tumor cells to glycolytic inhibitors. Biochemistry 40:5542–5547.

Liu L, Yang M, Kang R, Wang Z, Zhao Y, Yu Y, Xie M, Yin X, Livesey KM, Lotze MT, Tang D, Cao L. 2011. HMGB1-induced autophagy promotes chemotherapy resistance in leukemia cells. Leukemia 25:23–31.

Lopez G, Torres K, Liu J, Hernandez B, Young E, Belousov R, Bolshakov S, Lazar AJ, Slopis JM, McCutcheon IE, McConkey D, Lev D. 2011. Autophagic survival in resistance to histone deacetylase inhibitors: novel strategies to treat malignant peripheral nerve sheath tumors. Cancer Res 71:185–196.

Matsushita N, Takami Y, Kimura M, Tachiiri S, Ishiai M, Nakayama T, Takata M. 2005. Role of NAD-dependent deacetylases SIRT1 and SIRT2 in radiation and cisplatin-induced cell death in vertebrate cells. Genes Cells 10:321–332.

Moreno-Sanchez R, Rodriguez-Enriquez S, Marin-Hernandez A, Saavedra E. 2007. Energy metabolism in tumor cells. FEBS J 274:1393–1418.

Morimoto H. 1989. [Synthesis and biochemical actions of idebenone and related compounds. Ubiquinone and related compounds, XL]. Naturwissenschaften 76:200–205.

Nemoto S, Fergusson MM, Finkel T. 2004. Nutrient availability regulates SIRT1 through a forkhead-dependent pathway. Science 306:2105–2108.

O'Donovan TR, O'Sullivan GC, McKenna S. 2011. Induction of autophagy by drug-resistant esophageal cancer cells promotes their survival and recovery following treatment with chemotherapeutics. Autophagy 7(6). [Epub ahead of print] PMID:21325880

Oh WK, Cho KB, Hien TT, Kim TH, Kim HS, Dao TT, Han HK, Kwon SM, Ahn SG, Yoon JH, Kim YG, Kang KW. 2010. Amurensin G, a potent natural SIRT1 inhibitor, rescues doxorubicin responsiveness via down-regulation of multidrug resistance 1. Mol Pharmacol 78:855–864.

Picard F, Kurtev M, Chung N, Topark-Ngarm A, Senawong T, Machado De Oliveira R, Leid M, McBurney MW, Guarente L. 2004. Sirt1 promotes fat mobilization in white adipocytes by repressing PPAR-gamma. Nature 429:771–776.

Ren JH, He WS, Nong L, Zhu QY, Hu K, Zhang RG, Huang LL, Zhu F, Wu G. 2010. Acquired cisplatin resistance in human lung adenocarcinoma cells is associated with enhanced autophagy. Cancer Biother Radiopharm 25:75–80.

Rodgers JT, Lerin C, Haas W, Gygi SP, Spiegelman BM, Puigserver P. 2005. Nutrient control of glucose homeostasis through a complex of PGC-1alpha and SIRT1. Nature 434:113–118.

Saunders LR, Verdin E. 2007. Sirtuins: critical regulators at the crossroads between cancer and aging. Oncogene 26:5489–5504.

Simonnet H, Alazard N, Pfeiffer K, Gallou C, Beroud C, Demont J, Bouvier R, Schagger H, Godinot C. 2002. Low mitochondrial respiratory chain content correlates with tumor aggressiveness in renal cell carcinoma. Carcinogenesis 23:759–768.

Singh KK, Russell J, Sigala B, Zhang Y, Williams J, Keshav KF. 1999. Mitochondrial DNA determines the cellular response to cancer therapeutic agents. Oncogene 18:6641–6646.

Sun Y, Liu JH, Jin L, Lin SM, Yang Y, Sui YX, Shi H. 2010. Over-expression of the Beclin1 gene upregulates chemosensitivity to anti-cancer drugs by enhancing therapy-induced apoptosis in cervix squamous carcinoma CaSki cells. Cancer Lett 294:204–210.

Tan AS, Berridge MV. 2004. Distinct trans-plasma membrane redox pathways reduce cell-impermeable dyes in HeLa cells. Redox Rep 9:302–306.

Vaquero A, Scher MB, Lee DH, Sutton A, Cheng HL, Alt FW, Serrano L, Sternglanz R, Reinberg D. 2006. SirT2 is a histone deacetylase with preference for histone H4 Lys 16 during mitosis. Genes Dev 20:1256–1261.

Vazquez-Martin A, Oliveras-Ferraros C, Menendez JA. 2009. Autophagy facilitates the development of breast cancer resistance to the anti-HER2 monoclonal antibody trastuzumab. PLoS ONE 4:e6251.

Wang T, Marquardt C, Foker J. 1976. Aerobic glycolysis during lymphocyte proliferation. Nature 261:702–705.

White E, DiPaola RS. 2009. The double-edged sword of autophagy modulation in cancer. Clin Cancer Res 15:5308–5316.